Marine Chemistry 242 (2022) 104121

Contents lists available at ScienceDirect

Marine Chemistry

journal homepage: www.elsevier.com/locate/marchem

Sources of polyamines in coastal waters and their links to phytoplankton

Qian Liu [a,b,c,*], Naoyoshi Nishibori [d], James T. Hollibaugh [c]

[a] State Key Laboratory of Satellite Ocean Environment Dynamics, Second Institute of Oceanography, Ministry of Natural Resources, Hangzhou 310012, China
[b] Key Laboratory of Marine Ecosystem Dynamics, Second Institute of Oceanography, Ministry of Natural Resources, Hangzhou 310012, China
[c] Department of Marine Sciences, University of Georgia, Athens, GA 30602-3636, USA
[d] Shikoku University Junior College, Ojin, Tokushima 771-1192, Japan

ARTICLE INFO

Keywords:
Polyamines
Diatoms
Picoeukaryotes
cyanobacteria
Dissolved organic nitrogen
DON
DOC

ABSTRACT

Polyamines are key components of labile dissolved organic nitrogen in coastal waters. They are found in all living organisms, which are the sources of dissolved organic matter in marine environments. The concentrations of dissolved polyamines are generally low and are controlled as much by production as by consumption. Understanding the dynamics of intracellular pools of polyamines could provide insight to their dynamics in the environment and their potential contribution to ecosystem processes. We measured the concentrations of 6 common polyamines (putrescine, cadaverine, norspermidine, spermidine, norspermine and spermine) extracted from particles in water samples collected on the continental shelf of the South Atlantic Bight (SAB). The total concentrations of extractable polyamines (EPs) decreased from inshore to the shelf-break of the SAB, following a pattern similar to chlorophyll *a* and opposite to salinity. The composition of EPs was highly correlated with the distribution of phytoplankton species assessed as the abundance of diatom 18S rRNA genes, and with densities of picoeukaryote, Synechococcus and Prochlorococcus cells, suggesting that phytoplankton are the primary source of EPs, followed by a freshwater or nearshore source. Our data suggest that putrescine, norspermidine and spermidine are released primarily from diatoms and picoeukaryotes, while Synechococcus and dinoflagellates are the likely sources of norspermine and spermine.

1. Introduction

Polyamines are aliphatic compounds with multiple amine groups covalently bonded to a carbon skeleton. They are found in cells of all organisms and function as growth stimulators, osmolytes and physiological buffers (Tabor and Tabor, 1985). Polyamines exist in free, conjugated and bound forms in cells. They bind to DNA, RNA, cell membranes, and are also found to be covalently attached to peptidoglycan in bacterial cell walls (Michael, 2018) or co-precipitated with silica during the formation of diatom cell walls (Kröger et al., 2000; Sumper and Kröger, 2004). Dissolved polyamines in the environment are preferentially assimilated by heterotrophic microorganisms as carbon (C) and nitrogen (N) sources, most likely due to their low molecular weight and high N:C ratios (Lee and Jørgensen, 1995; Liu et al., 2015). They can be degraded intracellularly with the amine groups released as NH_3 and the C skeleton oxidized for energy (Mou et al., 2011). The concentration of dissolved polyamines in seawater is typically at the nM level due to the rapid uptake by bacterioplankton (Nishibori et al., 2001, 2003; Lu et al., 2014; Liu et al., 2015); however, intracellular pools of polyamines are generally at the mM level, comparable to those of amino acids (Hamana and Matsuzaki, 1985; Cohen, 1997; Liu et al., 2016). Since intracellular polyamines are ultimately lost from cells to the environment as a consequence of cell death, viral lysis, grazing, etc., their composition may influence the composition of bioavailable polyamines in the environment.

Major intracellular polyamines in prokaryotic and eukaryotic cells include the diamines cadaverine (CAD) and putrescine (PUT), the triamines norspermidine (NSPD) and spermidine (SPD), and the tetramines norspermine (NSPM) and spermine (SPM; e.g., Hamana and Matsuzaki, 1985, Cohen, 1997; Nishibori and Nishijima, 2004; Liu et al., 2016; Michael, 2018). Phytoplankton have been considered as the major sources of dissolved polyamines in marine environments, since several studies have established significant correlations between the turnover or concentration of dissolved polyamines and chlorophyll *a* (Chl *a*) concentrations (Lee and Jørgensen, 1995; Nishibori et al., 2001, 2003; Liu et al., 2015; Liu et al., 2016). The compositions and concentrations of

* Corresponding author at: State Key Laboratory of Satellite Ocean Environment Dynamics, Second Institute of Oceanography, Ministry of Natural Resources, Hangzhou 310012, China.
E-mail address: liuqian@sio.org.cn (Q. Liu).

https://doi.org/10.1016/j.marchem.2022.104121
Received 3 February 2022; Received in revised form 20 April 2022; Accepted 24 April 2022
Available online 29 April 2022
0304-4203/© 2022 Elsevier B.V. All rights reserved.

intracellular polyamines differ among phytoplankton species (Hamana and Matsuzaki, 1982, 1985; Nishibori and Nishio, 1997; Nishibori and Nishijima, 2004; Liu et al., 2016), suggesting that the mix of dissolved polyamines available in the environment may be controlled by phytoplankton community composition. Previous work shows that PUT and SPD are the most common polyamines, ubiquitously distributed in all phytoplankton species. NSPD is typically less abundant in marine environments but has been found in diatoms, cyanobacteria, red algae and some dinoflagellates. CAD and NSPM are relatively rare, and only occasionally detected in diatoms, Chlorophyta, dinoflagellates and red algae. SPM is the major polyamine in red algae, and is less commonly found in other eukaryotic algae (e.g., Hamana and Matsuzaki, 1985; Nishibori and Nishio, 1997; Lu and Hwang, 2002; Lin and Lin, 2019). PUT is also closely associated with the growth of higher plants (Shen and Galston, 1985) and some freshwater algae (Kotzabasis, 1994; Theiss et al., 2002). Spatio-temporal variation in phytoplankton distribution may thus cause differences in the supply and relative abundance of dissolved free polyamines that are available to bacterioplankton.

The South Atlantic Bight (SAB) extends from North Carolina to Florida, inshore of the Gulf Stream, and includes both shelf and slope waters. Nearshore waters of the SAB are influenced by river runoff and tidal exchange with extensive salt marshes and estuaries. Offshore waters are oceanic and influenced by the Gulf Stream (Liu et al., 2015). Temperature (T), salinity (S), Chl *a* concentration, turbidity and thus photic zone depth and nutrients vary spatially and temporally from inshore to offshore (Liu et al., 2015, 2018).

We measured the concentrations and turnover rates of dissolved polyamines in the SAB on two cruises during 2011 (Lu et al., 2014; Liu et al., 2015). The low concentrations (nM) of dissolved polyamines and the rapid turnover rates measured suggest that polyamines are important sources of organic N for bacterioplankton production. Uptake rates of polyamines correlated closely with Chl *a* concentration, suggesting that polyamine fluxes could be tied to phytoplankton distributions (Liu et al., 2015). Moreover, individual polyamines (PUT, SPD and SPM) showed distinct patterns of concentrations and turnover rates, further implying spatial variability in their sources and sinks.

We followed our work on dissolved polyamines in 2011 with four cruises to the SAB in 2014, measuring concentrations and compositions of polyamines in suspended particulate material. We determined concentrations of Chl *a* and quantified the major phytoplankton species present in our samples. We tested the hypothesis that phytoplankton are the major source of these compounds and that the cycling of dissolved polyamines is linked closely to their abundance in phytoplankton.

2. Materials and methods

2.1. Sample collection

Seawater samples were collected on four cruises of the *R/V Savannah* on April 2–6, July 15–19, September 24–30, and November 3–6, 2014 at stations across the SAB from inshore to slope waters (Fig. 1 and Supplementary Table S1). Since the shelf region is shallow (<50 m depth) and generally well-mixed (Atkinson, 1977), samples were only collected from the surface (SW) and the bottom water (BW) layers at inshore, nearshore and mid-shelf stations (Supplementary Table S1). Samples were collected at shelf-break stations (depth > 200 m) from depths of 10 m, 200 m (mid-depth water, MW) and 400 m (Fig. 1 and Supplementary Table S1). Samples were collected using 12 L Niskin bottles mounted on a rosette frame equipped with a Sea-Bird SBE 25 CTD. Samples were also collected during high and low tide at the inshore stations ALTES, DOBES and SAPES in September and from waters upstream of Stn ALTES (Stn ALUp_S) in November (Fig. 1 and Supplementary Table S1) to

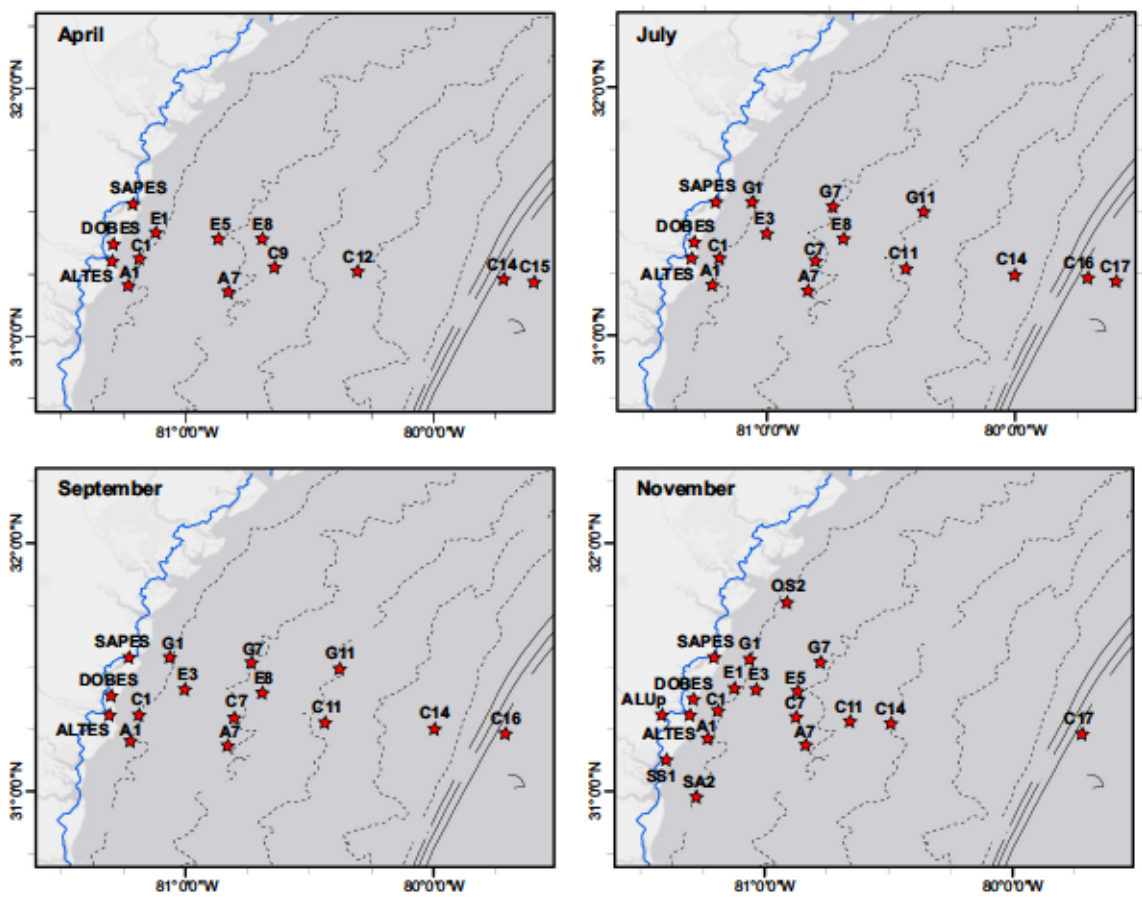

Fig. 1. Sampling locations on different cruises at the South Atlantic Bight. The map is modified from Liu et al. (2018).

characterize the riverine end-member of shelf water.

The composition of particles in our samples was assessed by flow cytometry. One milliliter of seawater from each sample was placed into a 1.2-mL cryogenic vial and 5 μL of 25% EM grade glutaraldehyde was added to a final concentration of 0.125%. The sample was mixed vigorously 5 times and left at room temperature in the dark for 10 min, then frozen in liquid nitrogen for subsequent analysis of the abundance and characteristics of particles via flow cytometry. DNA extraction, concentrations of Chl *a* and dissolved inorganic nitrogen (DIN, including nitrate, nitrite and ammonium), and bacterial abundance were analyzed as described in Liu et al. (2018). Temperature, salinity, photosynthetically active radiation (PAR), Relative Fluorescence (RF) and the concentration of dissolved oxygen (DO) were measured by sensors on the CTD.

2.2. Extraction and measurement of particulate polyamines

Seawater collected at each sampling site (~0.3 L) was filtered on board through 25 mm diameter, combusted GF/F filters (Whatman, USA). The wet filter was placed in a 15-mL falcon tube, 1 mL of ice-cold 6% perchloric acid (PCA) was added, then the tube was frozen at −20 °C until laboratory analysis (Lu and Hwang, 2002; Liu et al., 2016). A blank filter treated similarly served as a negative control.

Samples were thawed at room temperature in the laboratory, another 1 mL of 6% PCA was added, and the vial vortexed thoroughly to ensure that cells on the filter were mixed into the PCA. The mixture was sonicated for 30 min and centrifuged at 3000 x g for 10 min. A total of 1.8 mL of supernatant was transferred to a 2-mL centrifuge tube, which was centrifuged at 10,000 x g for 15 min. The supernatant (~1.5 mL) was collected and stored at −80 °C until analysis. The concentrations of polyamines in the extract were measured by high-performance liquid chromatography (HPLC) as described in Liu et al. (2016). Controls consisting of blank filters were prepared and processed as above. Six common polyamines, including PUT, CAD, NSPD, SPD, NSPM and SPM, were quantified. Total concentration of extractable polyamines was estimated by adding the concentrations of individual polyamines.

2.3. Abundances of Synechococcus, Prochlorococcus and picoeukaryote cells

Synechococcus, Prochlorococcus and picoeukaryotes were enumerated by dual beam flow cytometry on a modified Coulter-EPICS 753 flow cytometer (Beckman Coulter, Fullerton, CA, USA; Binder et al., 1996; Burbage and Binder, 2007). The flow cytometer was equipped with a 6 W argon laser (power 1000 mW, at 488 nm). We added 2 μL of 0.92 μm yellow-green fluorescent beads (Fluoresbrite™; Polysciences, PA, USA; Crosbie and Furnas, 2001) to a 0.9 mL subsample as an internal standard. Samples were run at an infusion rate of 5–10 μL min^{-1} depending on abundance of cells in the sample, and a minimum of 20,000 particles were recorded. Two light scatter signals (side scatter and forward scatter) and two fluorescence signals (red fluorescence from chlorophyll, wavelength > 650 nm; orange fluorescence from phycoerythrin, wavelength: 564–606 nm) were recorded on four-decade logarithmic scales (1, 10, 100 and 1000; Olson et al., 1993). The abundance of Synechococcus cells was quantified on an orange fluorescence versus side-scatter biplot, while Prochlorococcus and photosynthetic picoeukaryotes were quantified on red fluorescence versus forward light-scatter biplots (Olson et al., 1993).

2.4. Diatom 18S rRNA gene abundance

We quantified the abundance of diatom 18S rRNA genes as an estimate of the total abundance diatoms in our samples. Standards for qPCR quantification of diatom 18S rRNA gene were prepared as follows. The diatom *Thalassiosira pseudonana* (CCMP1335) was purchased from the National Center for Marine Algae and Microbiota (NCMA) and inoculated into 100 mL of f/2 culture media. The culture was grown and transferred axenically as described in Liu et al. (2016). The culture was harvested at the end of exponential growth and fixed with acidified Lugol's iodine solution (20 g potassium iodide, 10 g iodine, 20 g concentrated acetic acid in 200 mL distilled water; ~0.2–0.5 mL). The fixed sample was centrifuged at 3,000 x g for 15 min at 12 ± 1 °C. The supernatant was removed and the cell pellets resuspended in 1.5 mL of sterile artificial seawater and transferred to a 1.5 mL centrifuge tube, followed by centrifugation at 10,000 x g for 15 min at 12 ± 1 °C. The supernatant was removed and the cells were centrifuged again at 10,000 x g for 15 min to remove any remaining supernatant. The pellet was frozen at −80 °C for 15 min, then resuspended in 400–600 μL of lysis buffer (PCR buffer 1×, NP40 0.5%, Tween 20 0.5% and proteinase K 0.1 mg mL^{-1}) to a final concentration of $1x10^5$-$2x10^5$ cells mL^{-1}. The cells were sonicated and incubated at 55 ± 1 °C for 2 h and vortexed at intervals of ~30 min. DNA was extracted from the lysate following Bano and Hollibaugh (2000). An 18S rDNA gene fragment 1040 bp long was amplified from the DNA extracted from *T. pseudonana* with primers Prim-A (CCGAATTCGTCGACAACCTGGTTGATCCTGCCAGT) and Neid-54 (CATAACGTAACACTGCCG) following the same PCR conditions as Nguyen et al. (2011): denaturing the DNA at 95 °C for 4 min, then performing 24 PCR cycles: denaturing at 94 °C for 45 s, annealing for 30 s at 58 °C and extension at 72 °C for 30 s, with a final extension step at 72 °C for 2 min. Ten microliters of PCR product was analyzed on 2% (*w/v*) agarose gel in TBE buffer (50 mM Tris-HCl pH 8.0, 50 mM boric acid, 1 mM EDTA). The band containing the amplicon was sliced from the gel and purified using a DNA clean-up kit, then quantified spectrophotometrically. Gene concentrations in the standard were estimated from measured DNA concentrations, plasmid length and insert sequence length.

Diatom 18S rRNA genes in DNA extracted from field samples were quantified by PCR using primers 528F (GCGGTAATTCCAGCTCCAA) and 650R (AACACTCTAATTTTTTCACAG; Nguyen et al., 2011). Twenty-four μL of master mix containing 1 μL of each primer (final concentration: 0.3 μM), 9.5 μL H_2O and 12.5 μL of SYBR Green dye (Qiagen Quantitech SYBR Green Kit) and 1 μL of environmental DNA template was added to each well. qPCR amplification was conducted using an iCycler iQTM Real-Time qPCR detection system (BioRad) with conditions as follows: initial denaturation of DNA at 95 °C for 15 min; 40 cycles with 15 s denaturation at 94 °C, followed by 30 s annealing at 50 °C and 30 s extension at 72 °C (Nguyen et al., 2011). Standard curves (dilutions of the standard from above containing 9.73, $9.73x10^2$, $9.73x10^4$, $9.73x10^6$, and $9.73x10^7$ copies μL^{-1}) were linear and qPCR efficiency ranged from 81.9–90.3% (R^2 = 0.994, S.D. = 0.004). Concentrations of diatom 18S rRNA genes in field samples were estimated from concentrations of diatom 18S rRNA gene in the template, the total volume of DNA extract per sample, the volume filtered for each sample, and we assume 100% extraction efficiency.

2.5. Statistical analysis

Redundancy analysis (RDA) was applied to identify environmental factors and phytoplankton groups that might influence EP distributions. Linear relationships are assumed between response and explanatory variables in RDA (Legendre and Legendre, 2012). The log-transformed environmental data (temperature, salinity, bacterial abundances, and concentrations of DO, Chl *a* and DIN) and phytoplankton abundances measured during the four cruises were analyzed with 999 Monte-Carlo permutations using the software package CANOCO (5.1; ter Braak and Smilauer, 2002). Pearson Product Moment Correlations were used to investigate correlations among concentrations of individual and total extractable polyamines, environmental variables and abundances of phytoplankton.

3. Results

3.1. Environmental characteristics and phytoplankton composition of the study region

The water column was well-mixed at stations <50 m deep and the mixed layer depth at shelf-break stations was ~50 m. Salinity increased from inshore to the shelf-break during all sampling seasons (Figs. 2, S1). The inshore stations (ALTES, DOBES, SAPES and SS1) are influenced by river inflow, having lower S (Fig. 2). Salinity at station ALTES, located at the mouth of the Altamaha River, fluctuated significantly between high tide, when surface water (SW) and bottom water (BW) salinity was 31.8, and low tide when SW salinity was 15.9 and BW salinity was 16.3. Salinity varied over a narrower range at stations DOBES, SAPES and SS1 (29.2–32.4; Fig. 2c). Salinity at Stn ALUp_S was approximately 3 (Fig. 2d). Salinity was lowest at inshore and nearshore stations in April due to stronger riverine inflow (Fig. S1). Temperature also increased from inshore to the shelf-break, except in July (Fig. S1). Water temperature was lowest in all regions in April (12.1–24.8 °C) and peaked in July at 23.9–29.5 °C from inshore to the mid-shelf region (Fig. S1). The concentration of Chl *a* decreased from inshore to mid-shelf and then became relatively uniform at the shelf break (Fig. 2, Fig. S1).

The distributions of diatom 18S rRNA genes and the abundance of picoeukaryotes displayed similar patterns, decreasing from inshore to the shelf-break, except for picoeukaryotes in September (Fig. 3a). The abundances of picoeukaryotes and diatom 18S rRNA genes were well correlated (Pearson Product Moment Correlation, $R = 0.44$, $p < 0.0001$), and both were positively correlated with concentrations of Chl *a* ($p < 0.0001$) and DIN ($p < 0.01$) and negatively related with S ($p < 0.001$, $n = 121$; Table 1). Diatom 18S rRNA genes were most abundant in samples from the inshore region, reaching over 10^9 copies L^{-1}, followed by the abundances of Synechococcus ($6.39 \times 10^7 \pm 3.50 \times 10^7$ cells L^{-1}), picoeukaryotes ($1.73 \times 10^7 \pm 8.52 \times 10^6$ cells L^{-1}) and Prochlorococcus ($1.50 \times 10^7 \pm 2.55 \times 10^7$ cells L^{-1}; Fig. 3b). Synechococcus was generally abundant in nearshore ($1.63 \times 10^8 \pm 8.49 \times 10^7$) and mid-shelf regions ($1.37 \times 10^8 \pm 7.96 \times 10^7$), comparable to the abundance of diatom 18S rRNA genes (nearshore:$7.26 \times 10^8 \pm 6.15 \times 10^8$; mid-shelf: $2.78 \times 10^8 \pm 2.37 \times 10^8$; Fig. 3b). Prochlorococcus was the dominant phytoplankton group at the shelf-break ($1.37 \times 10^8 \pm 6.96 \times 10^7$; Fig. 3).

3.2. Distributions of extractable polyamines in the SAB

The total concentration of extractable polyamines (EPs) decreased from inshore to shelf-break stations on all cruises, with a distribution similar to the concentration of Chl *a*, but opposite to salinity (Fig. 2). Note that separate analysis of differences in EPs between surface and bottom waters in coastal waters (inshore, nearshore and mid-shelf waters) of the SAB is not included in this study due to their similarity

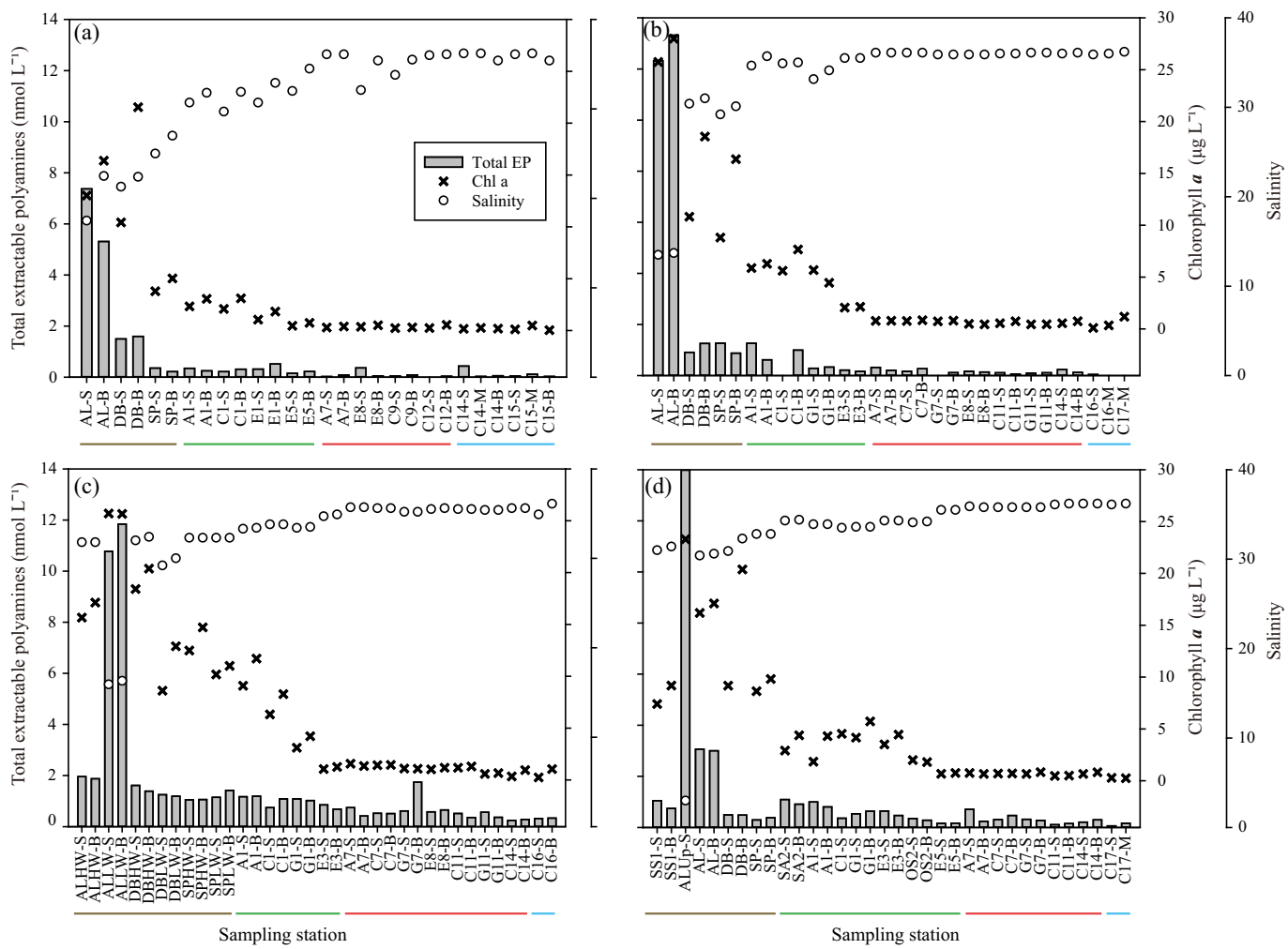

Fig. 2. Distributions of salinity, concentrations of chlorophyll *a* (μg L^{-1}) and total extractable polyamines (nmol L^{-1}) during cruises in (a) April, (b) July, (c) September and (d) November in the South Atlantic Bight. The sampling stations were classified into different regions (brown, inshore; green, nearshore; red, mid-shelf; blue, shelf-break) based on their locations referred to Fig. 1 and Supplementary Table S1. (For interpretation of the references to colour in this figure legend, the reader is referred to the web version of this article.)

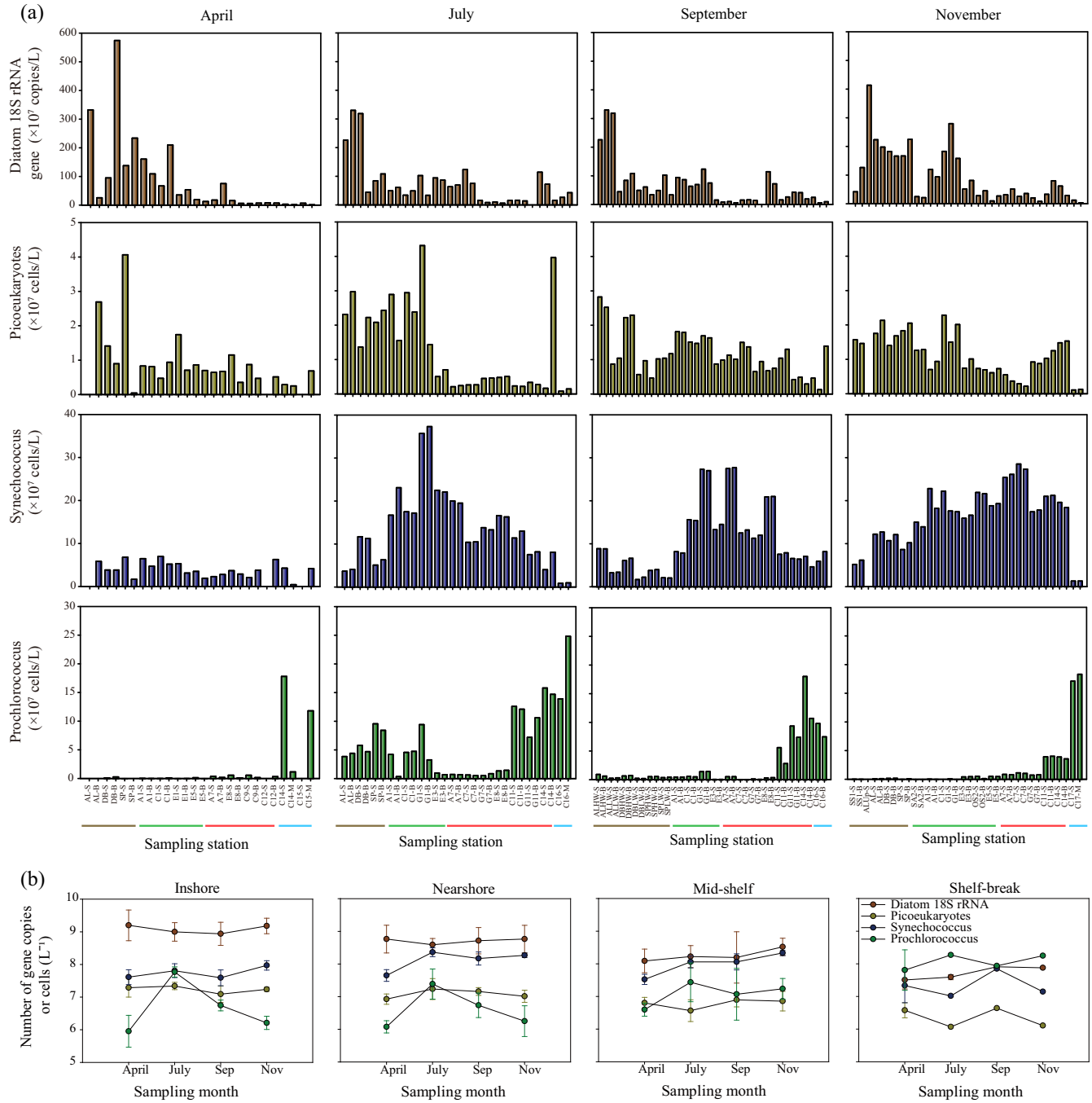

Fig. 3. (a) Distribution patterns of numbers of diatom 18S rRNA gene and cell densities of picoeukaryotes, Synechococcus and Prochlorococcus in samples collected at the South Atlantic Bight during different sampling months. The sampling stations were classified into different regions (brown, inshore; green, nearshore; red, mid-shelf; blue, shelf-break) based on their locations referred to Fig. 1 and Supplementary Table S1. (b) Seasonal variations of the means of log-transformed gene copy or cell densities of diatom 18S rRNA, picoeukaryotes, Synechococcus and Prochlorococcus at inshore, nearshore, mid-shelf and shelf-break regions of the South Atlantic Bight. Error bars represent the standard deviations of means of each variable. (For interpretation of the references to colour in this figure legend, the reader is referred to the web version of this article.)

caused by the relatively well-mixed waters and similar environmental characteristics of these two layers. The average concentration of total EPs (all cruises) was 2.9 ± 3.8 nmol L^{-1} (mean ± SD) at inshore stations (excluding data from Stn ALUp_S), decreasing to values <1 nmol L^{-1} at other regions (Fig. 2). Total EP concentrations were greatest in samples collected from Altamaha River stations ALTES (7.1 ± 4.6 nmol L^{-1}) and ALUp_S (33.5 nmol L^{-1}; Fig. 2). Total EP concentrations measured at Stn ALTES during low tide were 5 times higher than those measured during high tide (Fig. 2c).

The composition of EPs changed from inshore to shelf-break stations (Fig. 4). The distribution of extractable PUT (ePUT), eNSPD and eSPD pools followed a pattern similar to that of total EPs, decreasing toward the shelf-break (Fig. 4). ePUT, eNSPD and eSPD were the major EPs present at inshore stations, with total EP concentration dominated by eSPD (mean ± SD, % of total EP: 54 ± 14%; Fig. 4). ePUT was the primary EP at stations ALTES (SW: 5.9 nmol L^{-1}, 80%; BW: 4.0 nmol L^{-1}, 75%) and DOBES (SW: 0.7 nmol L^{-1}, 45%; BW: 1.2 nmol L^{-1}, 74%) in April, and at Stn ALUp_S in November (21 nmol L^{-1}, 63%; Fig. 4). The concentrations of eCAD, eNSPM and eSPM did not have a regular pattern of distribution in the SAB. eCAD was detected ubiquitously in

Table 1
Pearson Product Moment Correlations were established among concentrations of total/single extractable polyamines (PUT, putrescine; CAD, cadaverine; NSPD, norspermidine; SPD, spermidine; NSPM, norspermine; SPM, spermine; total EPs, total extractable polyamines), environmental variables (T, temperature; S, salinity; Chl *a*, chlorophyll *a*; DIN, concentration of dissolved inorganic nitrogen; bacteria, bacterial 16S rRNA gene abundance; DO, concentrations of dissolved oxygen) and abundances of phytoplankton (Diatoms, diatom 18S rRNA gene; Picoeuk, picoeukaryote; Syne, Synechococcus; Prochl, Prochlorococcus). Data were log-transformed before the analysis. The colour gradients represent the ranges of *p* values.

All Sampling Months ($n = 128$)		Extractable Polyamines (EPs)							Environmental Variables						Phytoplankton			
		PUT	CAD	NSPD	SPD	NSPM	SPM	Total EPs	T	S	Chl *a*	DIN	Bacteria	DO	Diatoms	Picoeuk	Syne	Prochl
Extractable Polyamines (EPs)	PUT	1	−0.02	0.77	0.83	−0.16	0.07	0.90	−0.15	−0.93	0.52	0.56	0.33	0.06	0.33	0.25	−0.20	−0.09
	CAD	−0.02	1	0.16	0.10	0.14	0.11	0.19	0.23	0.03	0.10	0.16	0.17	−0.37	−0.13	0.10	−0.13	0.06
	NSPD	0.77****	0.16	1	0.97	−0.16	0.10	0.93	0.07	−0.80	0.73	0.77	0.47	−0.23	0.42	0.39	−0.22	−0.02
	SPD	0.83****	0.10	0.97****	1	−0.11	0.05	0.97	0.02	−0.83	0.75	0.73	0.49	−0.14	0.46	0.42	−0.12	−0.10
	NSPM	−0.16	0.14	−0.16	−0.11	1	0.34	−0.11	0.13	0.17	−0.20	−0.33	−0.10	0.04	−0.21	0.06	0.44	−0.13
	SPM	−0.07	0.11	−0.10	−0.05	0.34***	1	−0.03	0.21	0.10	−0.15	−0.18	−0.09	−0.10	−0.09	−0.09	0.24	−0.05
	Total EPs	0.90****	0.19*	0.93****	0.97****	−0.11	0.03	1	−0.02	−0.86	0.76	0.74	0.50	−0.13	0.45	0.44	−0.16	−0.12
Environmental Variables	T	−0.15	0.23*	0.07	0.02	0.13	0.21	−0.02	1	0.18	−0.07	−0.04	0.04	−0.78	−0.25	−0.10	0.25	0.65
	S	0.93***	0.03	0.80****	0.83***	0.17	0.10	0.86****	0.18*	1	−0.54	−0.57	−0.37	−0.05	−0.40	−0.31	0.29	0.16
	Chl *a*	0.52****	0.10	0.73***	0.75***	−0.20*	0.15	0.76***	0.07	0.54****	1	0.72	0.69	−0.16	0.67	0.62	−0.04	−0.27
	DIN	0.56****	0.16	0.77***	0.73***	0.33**	0.18	0.74***	−0.04	0.57***	0.72****	1	0.29	−0.29	0.36	0.29	−0.53	−0.09
	Bacteria	0.33***	0.17	0.47****	0.49****	−0.10	0.09	0.50****	0.04	0.37****	0.69****	0.29**	1	−0.07	0.49	0.44	0.05	−0.23
	DO	0.06	0.37****	0.23**	−0.14	0.04	0.10	−0.13	0.78****	−0.05	−0.16	0.29**	−0.07	1	0.15	−0.06	0.04	−0.44
Phytoplankton	Diatoms	0.33***	−0.13	0.42****	0.46****	−0.21*	0.09	0.45****	0.25**	0.40****	0.67****	0.36****	0.49****	0.15	1	0.44	0.16	−0.31
	Picoeuk	0.25**	0.10	0.39****	0.42****	0.06	0.09	0.44****	−0.10	0.31***	0.62****	0.29**	0.44****	−0.06	0.44****	1	0.30	−0.26
	Syne	−0.20*	−0.13	−0.22*	−0.12	0.44****	0.24**	−0.16	0.25**	0.29**	−0.04	0.53****	0.05	0.04	0.16	0.30***	1	−0.08
	Prochl	−0.09	0.06	−0.02	−0.10	−0.13	0.05	−0.12	0.65****	0.16	0.27**	−0.09	−0.23	0.44***	0.31**	−0.26*	−0.08	1

**** $p \leq 0.0001$.
*** $0.0001 < p \leq 0.001$.
** $0.001 < p \leq 0.01$.
* $0.01 < p < 0.05$.

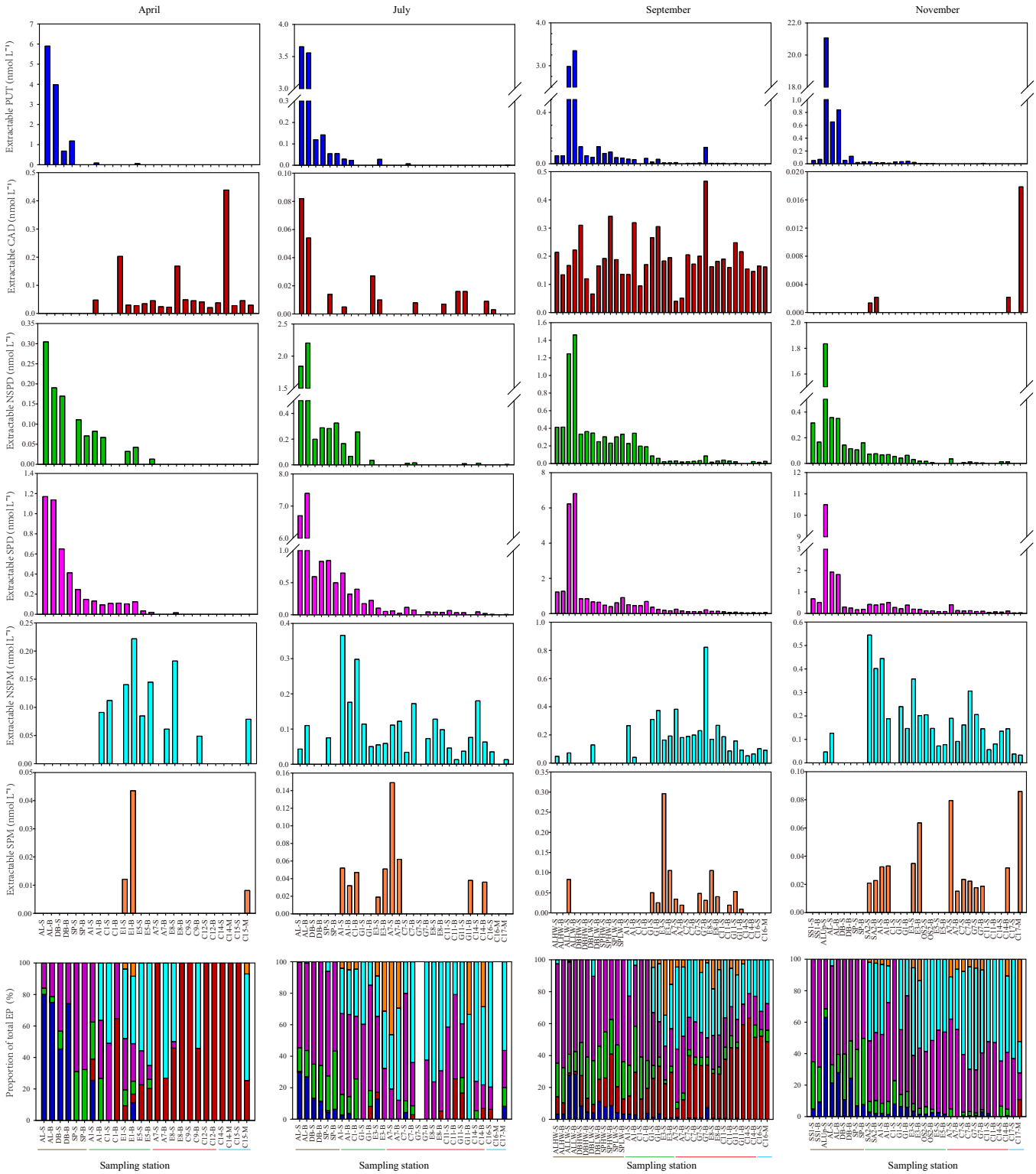

Fig. 4. Concentrations of extractable putrescine (PUT), cadaverine (CAD), norspermidine (NSPD), spermidine (SPD), norspermine (NSPM) and spermine (SPM), and proportions of each polyamine compound at sampling stations in April, July, September and November in the South Atlantic Bight. The sampling stations were classified into different regions (brown, inshore; green, nearshore; red, mid-shelf; blue, shelf-break) based on their locations referred to Fig. 1 and Supplementary Table S1. (For interpretation of the references to colour in this figure legend, the reader is referred to the web version of this article.)

September, when it was a major component of EPs (Fig. 4). It was detected sporadically in samples collected during other months, but became the primary EP at mid-shelf and shelf-break regions in April (Fig. 4). eNSPM and eSPM were rarely detected at inshore stations compared to other regions and the latter was detected randomly in the SAB (Fig. 4).

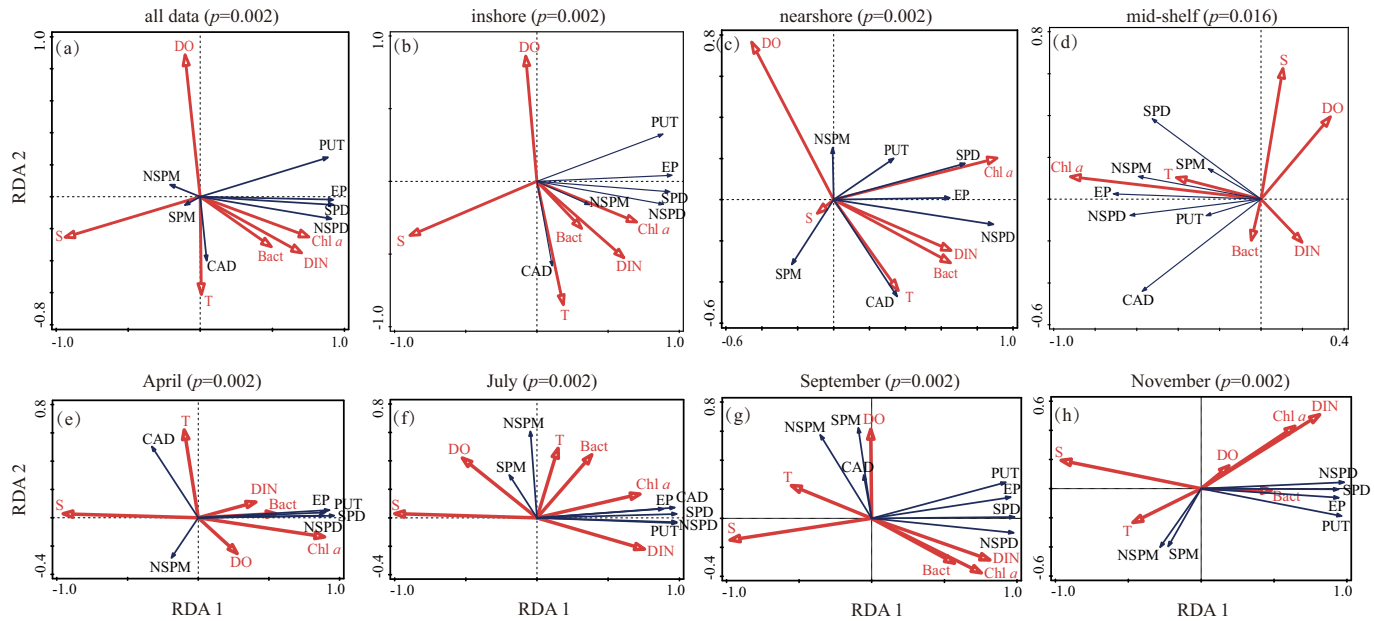

Fig. 5. RDA analysis of the relationship between distributions of total/single extractable polyamines (EPs) and environmental variables with data from (a) all sampling stations and months, (b-d) inshore, nearshore and mid-shelf during all sampling months, (e-h) April, July, September and November on the transect of the South Atlantic Bight. Data were log-transformed before the analysis. PUT, putrescine; CAD, cadaverine; NSPD, norspermidine; SPD, spermidine; NSPM, norspermine; SPM, spermine; T, temperature; S, salinity; Chl *a*, chlorophyll *a*; DIN, dissolved inorganic nitrogen; DO, dissolved oxygen; Bact, bacterial 16S rRNA gene.

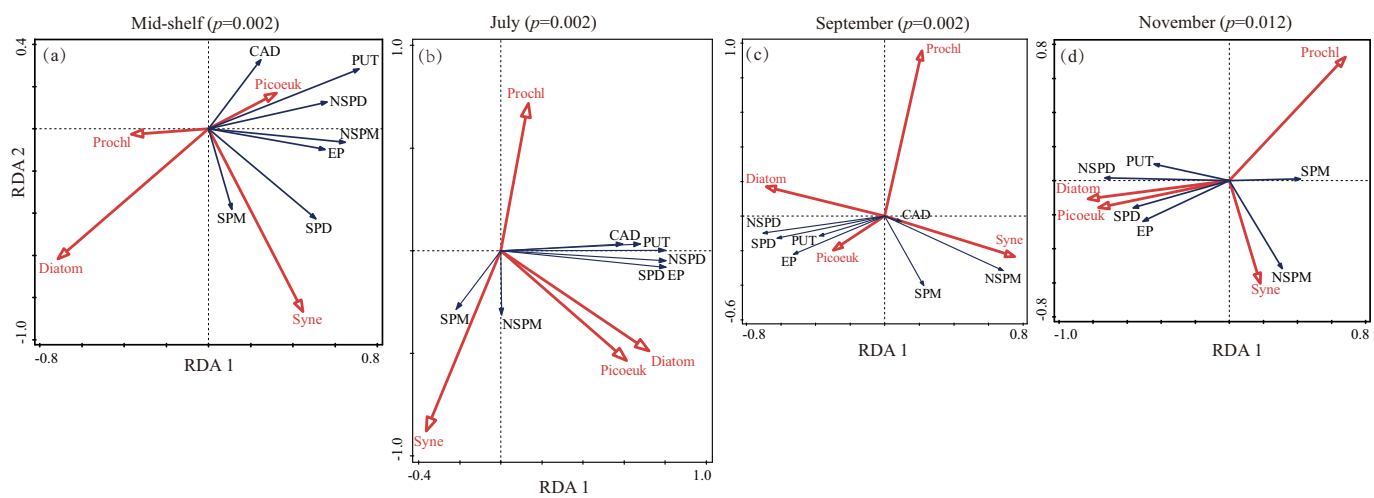

Fig. 6. RDA analysis of the relationship between distributions of total/single extractable polyamines (EPs) and phytoplankton abundances with data from (a) mid-shelf stations during all sampling months and (b-d) sampling stations in (b) July, (c) September and (d) November through the transect of the South Atlantic Bight. Analyses with *p*-value less than 0.05 are shown. Data were log-transformed before the analysis. PUT, putrescine; CAD, cadaverine; NSPD, norspermidine; SPD, spermidine; NSPM, norspermine; SPM, spermine; Picoeuk, picoeukaryotes; Syne, Synechococcus; Prochl, Prochlorococcus.

3.3. Environmental correlates of EP distributions

The RDA analysis of the distribution of total and individual EPs at all stations during all months captured 52.0% of the variation explained by environmental variables. RDA 1 captured 48.4% of the variation, while adding RDA 2 only increased the variance explained by 3.6% ($n = 128$, $p = 0.002$; Fig. 5a and Supplementary Table S2). Concentrations of total EPs, ePUT, eNSPD and eSPD clustered strongly on RDA 1 ($p < 0.0001$; Fig. 5a and Table 1). They were negatively correlated with S and varied positively with concentrations of Chl *a*, DIN and bacterial abundance ($p < 0.001$; Fig. 5a and Table 1); however, the variables S and Chl *a* concentration explained a total of 46.4% of the variance on RDA 1. Adding concentrations of DIN and bacterial abundance to the analysis did not significantly increase the amount of variance explained. Variation of ePUT pools correlated more strongly with S ($R = -0.93$) than did variation in eNSPD ($R = -0.80$) or eSPD ($R = -0.83$) pools (Table 1). eCAD ($R = 0.23$) and eSPM ($R = 0.21$) pools were positively correlated with T ($p = 0.01$) and the former inversely correlated with DO ($R = -0.37$, $p < 0.0001$). The concentration of eNSPM was weakly and inversely correlated with concentrations of Chl *a* ($R = -0.20$, $p = 0.023$) and DIN ($R = -0.33$, $p < 0.001$; Fig. 5a and Table 1).

We also performed RDA analyses on subsets of samples grouped by region (Figs. 5b-5d) or by month (Figs. 5e-5h and Supplementary Table S2). The spatial variation of environmental variables in each sampling month explained more of the variance in EP pools (RDA 1 eigenvalues: 0.547–0.666, correlation coefficient: 0.956–0.992; Figs. 5e-5h) than seasonal variation at each region (RDA 1 eigenvalues: 0.286–0.585, correlation coefficient: 0.677–0.956; Figs. 5b-5d and

Supplementary Table S2). The concentrations of total EPs, ePUT, eNSPD and eSPD were tightly clustered and correlated with S and concentrations of Chl *a* and DIN across the SAB on different cruises (Figs. 5e-5h and Supplementary Table S3). Analysis of the correlations based on seasonal variation in each region showed that the concentrations of total EPs, eNSPD and eSPD were mostly correlated with Chl *a* concentration on RDA 1 ($p < 0.001$; Figs. 5b-5d and Supplementary Table S4) at all regions, while ePUT concentrations were only associated with Chl *a* concentrations ($p < 0.001$) at the inshore region. Meanwhile, ePUT had a strong and negative correlation with S on RDA 1 ($p < 0.0001$; Fig. 5b and Supplementary Table S4).

3.4. Correlations between distributions of EPs and phytoplankton

RDA analyses were conducted to identify correlations between concentrations of EPs and the abundances of different phytoplankton groups (Fig. 6). When data were analyzed by region, seasonal variation in the concentrations of different EPs could only be explained by phytoplankton distributions at mid-shelf stations ($p = 0.002$; Fig. 6a and Supplementary Table S5). The concentrations of eSPD ($R = 0.60$, $p < 0.0001$), eNSPM ($R = 0.38$, $p < 0.01$) and eSPM ($R = 0.39$, $p < 0.01$) were positively correlated with the abundance of Synechococcus (Supplementary Table S4), which increased consistently from April to November in the mid-shelf region (Fig. 3). Although the seasonal variation of concentrations of different EPs were not explained in inshore ($p = 0.12$) and nearshore regions ($p = 0.05$; Supplementary Table S5), the concentration of eNSPD was correlated with the Prochlorococcus abundance at inshore stations ($R = 0.41$, $p < 0.05$; Supplementary Table S4); ePUT was correlated with the abundance of diatom 18S rRNA gene ($R = 0.38$, $p < 0.05$) in the nearshore region, while eNSPD, eSPD and total EPs were all strongly associated with the abundance of picoeukaryotes there ($R = 0.531$–0.57, $p < 0.001$; Supplementary Table S4).

The distribution of phytoplankton appeared to explain the spatial variation in EP composition in samples from the July ($p = 0.002$), September ($p = 0.002$) and November ($p = 0.006$) cruises (Figs. 6b-6d and Supplementary Table S5). Concentrations of eNSPD and eSPD were both correlated with the abundance of diatom 18S rRNA gene during these months ($R = 0.43$–0.56, $p < 0.01$) and with picoeukaryotes in July and November ($R = 0.50$–0.52, $p < 0.01$; Supplementary Table S3). The concentration of ePUT was only correlated with the abundances of diatom 18S rRNA gene in July ($R = 0.44$, $p < 0.01$) and November ($R = 0.41$, $p < 0.01$). eNSPM covaried with the abundance of Synechococcus in September ($R = 0.56$, $p < 0.001$) and November ($R = 0.39$, $p < 0.01$). CAD covaried with diatom 18S rRNA gene abundance in July ($R = 0.45$, $p < 0.01$), and with Prochlorococcus in April ($R = 0.63$, $p < 0.001$; Figs. 6b-6d and Supplementary Table S3).

4. Discussion

4.1. Potential sources of polyamines in the SAB

Polyamines can be released to the water column from phytoplankton, bacterioplankton, protists, and other larger organisms (Tabor and Tabor, 1985). Phytoplankton and bacterioplankton may be the major sources of polyamines to the euphotic zone due to their abundance and dominance of C and N fluxes there (Ducklow et al., 1993). We estimated the biomass of bacteria and of different groups of phytoplankton based on abundances we measured and mean biovolumes reported in the literatures (Strathmann, 1967; Bratbak, 1985; Verity et al., 1992; Partensky et al., 1999; Menden-Deuer and Lessard, 2000; Litchman et al., 2009; Moisan et al., 2010; Harrison et al., 2015) to evaluate their potential contributions to the dissolved organic carbon pool in SAB coastal waters (see Supplemental Methods and Materials; Supplementary Table S6). Unsurprisingly, the estimate shows that bacteria are major contributors to biomass in the SAB (~21%; Supplementary Table S6), emphasizing the role of bacteria in organic matter fluxes. However, higher total biomass of four groups of phytoplankton (Supplementary Table S6) and stronger correlations with concentrations of total EPs and Chl *a* in the SAB ($R_{\text{Chl } a} = 0.76$ vs $R_{\text{bacteria}} = 0.50$, $p < 0.0001$; Fig. 5; Tables 1, S3 and S4) imply that phytoplankton are likely the major sources of extractable polyamines in SAB waters. We note that seawater was filtered through GF/F filter (0.7 μm), which may only retain 70% to 80% of bacteria in estuarine, coastal, shelf and slope waters (Gasol and Morán, 1999), but since the intracellular pool of free polyamines (μmol/g wet weight) in bacteria is generally 0.1 to 0.01 that of phytoplankton (Hamana and Matsuzaki, 1985; Hosoya et al., 2006), bacterioplankton may not contribute significantly to the dissolved polyamine pool.

EPs may also be supplied to coastal waters by riverine input of terrestrial matter and organisms. The concentrations of total EPs measured in samples from the Altamaha River estuary (Stn ALTES), where the fertilizer and animal waste are the primary sources of nitrogen (Schaefer and Alber, 2005), are extremely high, and concentrations at Stn ALUp-S are relatively greater than predicted by Chl *a* concentration (Fig. 2). This suggests a terrestrial contribution to EP pools in the estuary. Two potential EP sources are considered: 1) polyamines may be rich in detrital particles which are brought in through riverine inflow; 2) the greater variability of salinity at Stn ALTES than that at Stn SAPES or at Stn DOBES (Fig. 2) may cause osmotic stress of oligo- and mesohaline phytoplankton and algae in estuaries, resulting in an increasing concentration of EPs acting as osmolytes in cells (Tabor and Tabor, 1985). The dissolved polyamine concentrations previously measured in the water at Stn ALTES were not significantly different from those at other estuarine sites with less freshwater impact (Liu et al., 2015), indicating the desorption from detrital particles in response to increased pH or salinity (Keil et al., 1997; Murrell and Hollibaugh, 2000) does not lead to the difference of EP pools in estuaries. Thus, the latter could be a major cause.

Of the individual extractable polyamines, ePUT is detected primarily at inshore and nearshore stations, and is more abundant in relatively fresher waters (S: 3–22.5; Fig. 4), suggesting a significant riverine or terrestrial source of ePUT. This is supported by the data indicating that PUT is abundant in plants and freshwater algae (Shen and Galston, 1985; Kotzabasis, 1994; Theiss et al., 2002). Concentrations of eSPD and eNSPD are more strongly correlated with Chl *a* than other EPs in all regions and sampling months (Fig. 5; Tables 1, S3 and S4), consistent with their ubiquitous distribution in algal cells (Hamana and Matsuzaki, 1985; Nishibori and Nishio, 1997; Lu and Hwang, 2002; Nishibori and Nishijima, 2004; Nishibori et al., 2006; Incharoensakdi et al., 2010; Liu et al., 2016).

Infrequent detection of CAD, NSPM and SPM in inshore waters (Fig. 4), and their weak correlations with Chl *a* (Table 1) suggest that their presence in intracellular pools could be influenced by environmental factors such as salinity or general physiological factors such as nutrient limitation (Yamaguchi et al., 2006; Incharoensakdi et al., 2010; Campestre et al., 2011; Sagor et al., 2013; Saha et al., 2015; Ahanger et al., 2019), or that they originate from specific groups of phytoplankton (Supplementary Tables S3 and S4; Hamana and Matsuzaki, 1985; Liu et al., 2016; Lin and Lin, 2019) or other biota (e.g., bacterioplankton; Knott, 2009). Intracellular concentrations of CAD and SPM both increase in plants (Campestre et al., 2011), and the latter also increases in cyanobacteria (Incharoensakdi et al., 2010) under salt stress. Genes in the SPM biosynthetic pathway, including SPM synthase gene and S-adenosylmethionine decarboxylase, are induced upon heat shock and SPM potentially protects plants from heat-induced damage (Sagor et al., 2013). Moreover, CAD and SPM production is enhanced for osmotic protection and salt stress tolerance (Yamaguchi et al., 2006; Saha et al., 2015; Ahanger et al., 2019). The positive correlations between concentrations of eCAD or eSPM with T detected in this study (Tables 1, Supplementary Table S3 and S4) suggest that T could be a stimulator of CAD and SPM production intracellularly. Variation of intracellular

NSPM concentrations in response to environmental stressors has not been studied as thoroughly, but our previous study (Liu et al., 2016) shows that the intracellular NSPM pool (amol cell^{-1}) increased with salinity in batch cultures of the diatom *T. pseudonana*, in contrast to PUT, SPD and NSPD concentrations, which decreased with increasing salinity. However, we did not find a direct connection between concentration of eNSPM and S. Thus, the presence of certain phytoplankton groups may be the source of NSPM in the SAB.

4.2. Extractable polyamine composition is related to phytoplankton distributions

In addition to environmental factors, variations in phytoplankton community composition may play a substantial role in the distribution of EPs in seawater, as different groups of phytoplankton contain different polyamines (Hamana and Matsuzaki, 1985; Nishibori et al., 2001; Liu et al., 2016; Schweikert and Burritt, 2015). Although the abundance of picoeukaryotes is generally lower than that of diatoms, Synechococcus, or Prochlorococcus (Fig. 3), they could be major primary producers due to their great biovolumes and fast growth rates (Supplementary Table S6; Worden et al., 2004). The low abundances of picoeukaryotes found both in this study and globally could be maintained by high virus lysis and grazing rates (Worden and Not, 2008; Kirkham et al., 2013). Thus, picoeukaryotes are also potentially major sources of polyamines to the environment.

The distributions of the cyanobacteria Synechococcus and Prochlorococcus were distinct from those of diatoms and picoeukaryotes, and from each other (Fig. 3). Synechococcus was detected in nearshore and mid-shelf stations as expected from their global distribution at low latitude (Rocap et al., 2003), while Prochlorococcus prefers oligotrophic mid-shelf and shelf-break waters (Partensky et al., 1999). Although we did not quantify all phytoplankton, those we measured likely represent the major groups present in SAB assemblages, based on an investigation in the adjacent Mid-Atlantic Bight (Makinen and Moisan, 2012), as well as the strong correlations we found between the abundance of diatom 18S rRNA gene or picoeukaryote and the concentration of Chl *a* (Table 1).

Correlations between concentrations of different EPs and measured abundances of phytoplankton groups (Fig. 6; Tables 1, Supplementary Tables S3 and S4) provide direct evidence for the feasibility of determining the potential availability of dissolved polyamines in seawater from phytoplankton distributions. Intracellular polyamine pools have been analyzed primarily in diatoms and picoeukaryotes (e.g., Chrysophyta and Chlorophyta) with PUT, NSPD and SPD as the most common compounds (Hamana and Matsuzaki, 1985; Hamana et al., 2013; Michael, 2016; Liu et al., 2016). We found that concentrations of ePUT, eNSPD and eSPD are closely correlated with abundances of these two phytoplankton groups (Fig. 6; Tables 1, Supplementary Tables S3 and S4), confirming that diatoms and picoeukaryotes are likely the major sources of these compounds in the SAB.

CAD, NSPM and SPM are less frequently detected in phytoplankton cells than PUT, SPD and NSPD (Hamana and Matsuzaki, 1985; Nishibori and Nishijima, 2004; Hamana et al., 2013; Liu et al., 2016; Lin and Lin, 2019). The concentration of eCAD correlated well with the distribution of Prochlorococcus in April (Supplementary Table S3), suggesting Prochlorococcus as the source of CAD. CAD is synthesized by lysine decarboxylase activity in plants and cyanobacteria (Incharoensakdi et al., 2010) and only occurs when lysine is abundant or PUT synthesis is blocked (Shah and Swiatlo, 2008). Comparison of lysine degradation pathways in Prochlorococcus and Synechococcus genomes indicates that the former always encodes lysine decarboxylase [EC:4.1.1.18], which is occasionally found in the latter (https://www.kegg.jp). Hosoya et al. (2005) also confirms that CAD is not detected in Synechococcus species.

NSPM contributes a relatively high proportion of EPs from nearshore to the shelf-break (36.2 ± 22.1%, mean ± S.D.; Fig. 4), and its concentration correlates with the abundance of Synechococcus (Tables 1, Supplementary Tables S3 and S4). However, NSPM has not been detected in cells of Synechococcus (Hosoya et al., 2005; Liu et al., 2016). Instead, it is abundant in dinoflagellate cells (Liu et al., 2016; Lin and Lin, 2019) and in the dissolved polyamine pool during a dinoflagellate bloom (Nishibori et al., 2003). We did not quantify dinoflagellates in our samples, but a survey of phytoplankton assemblages in the adjacent southern Mid-Atlantic Bight detected a pulse of dinoflagellates in summer (~10^5–10^6 cells L^{-1}), and the distribution pattern was similar to that of cyanobacteria (Makinen and Moisan, 2012). Thus, eNSPM may originate from dinoflagellates, despite the lack of direct evidence for a linkage. Due to the general lack of spermine synthase [EC:2.5.1.16], SPM only occurs in a few algal species, mostly in Raphidophyta, Rhodophyta and Chrysophyta (Hamana and Matsuzaki, 1985; Lin and Lin, 2019) and is detected occasionally in some species of prokaryotes (e.g., bacteria, cyanobacteria; Hosoya et al., 2005, 2006). The dominance of diatoms and picoeukaryotes in the SAB may explain the minor contribution of SPM to the total EP pool there.

4.3. Relationship between extractable polyamines and the cycling of dissolved polyamines in the SAB

Our previous study of the distribution and turnover rates of dissolved polyamines in the SAB (Liu et al., 2015) found a strong correlation between microbial uptake of polyamines and the concentration of Chl *a*. This correlation led us to hypothesize that phytoplankton were major sources of polyamines to SAB waters and that loss from phytoplankton cells controlled the availability of polyamines to bacterioplankton. Our finding here that phytoplankton are the major sources of extractable polyamines in the SAB supports this hypothesis.

Our previous study only measured the uptake rates of three readily available, radiolabeled polyamines (PUT, SPD and SPM) on cruises in April and October of 2011 (Liu et al., 2015). The October (2–6) 2011 cruise sampled the same season as the September of 2014 (24–30) cruise of the present study, allowing us to compare data from these cruises. With the caveat that the samples were taken two years apart, we found that the averaged uptake rates of dissolved SPD measured in each region of the SAB during 2011 cruises were linearly related to the mean size of extractable SPD pools measured at the same regions in 2014 (linear regression, $R^2 > 0.99$, $p < 0.05$; Fig. S1). Based on the strong correlation between concentrations of extractable SPD and Chl *a* that we found in 2014 ($R = 0.75$, $p < 0.0001$; Table 1), this relationship supports the conceptual model that microbial uptake of SPD was controlled by phytoplankton release. We found only a weak, or no, relationship for PUT and SPM, due to their sporadic occurrence in particulate pools in 2014 or in dissolved pools in 2011 (Fig. S2). Again, this affirms that SPD is phytoplankton origin in the SAB.

5. Conclusions

Our study suggests that phytoplankton are the major source of polyamines in the SAB, and likely elsewhere. Freshwater algae or terrestrial materials transported into the coastal zone by rivers may also contribute significantly to the particulate polyamine pool, especially of PUT in estuarine waters. The abundance and composition of the phytoplankton community is thus likely to control the composition of the dissolved polyamine pool directly. In turn, this affects the supply of polyamines to bacterioplankton. This study provides an insight into the dynamics of an intracellular pool of organic matter with rapid turnover in the environment, and could be the key to understand their bioavailability and involvement in the cycling of nutrient elements.

Author contributions

QL and JTH initiated and designed the research. QL collected the samples. QL and NN conducted the analyses of samples. QL wrote the

manuscript.

Funding

The research was funded by Scientific Research Fund of the Second Institute of Oceanography, MNR (grant No. HYGG1901), the National Natural Science Foundation of China (grants No. 42176038), the US National Science Foundation (NSF OCE 13-35838 to JTH) and the Project of State Key Laboratory of Satellite Ocean Environment Dynamics, Second Institute of Oceanography (No. SOEDZZ2204).

Declaration of Competing Interest

The authors declare they have no conflict of interest.

Acknowledgments

We thank the captain and crew of the R/V Savannah for their assistance with sampling during four cruises. We also would like to express our gratitude to Dr. Brian Binder from University of Georgia, USA for his assistance with our analysis of phytoplankton community composition by flow cytometry. We thank anonymous reviewers for constructive comments that improved an earlier version of this manuscript. This is contribution 1101 from the University of Georgia Marine Laboratory.

Appendix A. Supplementary data

Supplementary data to this article can be found online at https://doi.org/10.1016/j.marchem.2022.104121.

References

Ahanger, M.A., Qin, C., Maodong, Q., Dong, X.X., Ahmad, P., Abd_Allah, E.F., Zhang, L., 2019. Spermine application alleviates salinity induced growth and photosynthetic inhibition in *Solanum lycopersicum* by modulating osmolyte and secondary metabolite accumulation and differentially regulating antioxidant metabolism. Plant Physiol. Biochem. 144, 1–13.

Atkinson, L.P., 1977. Modes of gulf stream intrusion into the South Atlantic bight shelf waters. Geophys. Res. Lett. 4 (12).

Bano, N., Hollibaugh, J.T., 2000. Diversity and distribution of DNA sequences with affinity to ammonia-oxidizing bacteria of the ß subdivision of the class *Proteobacteria* in the Arctic Ocean. Appl. Environ. Microbiol. 66, 1960–1969.

Binder, B.J., Chisholm, S.W., Olson, R.J., Frankel, S.L., Worden, A.Z., 1996. Dynamics of picophytoplankton, ultra-phytoplankton and bacteria in the central equatorial Pacific. Deep-Sea Res. Part II Top. Stud. Oceanogr 43, 907–931.

Bratbak, G., 1985. Bacterial biovolume and biomass estimations. Appl. Environ. Microbiol. 49 (6), 1488–1493.

Burbage, C.D., Binder, B.J., 2007. Relationship between cell cycle and light-limited growth rate in oceanic Prochlorococcus (MIT9312) and Synechococcus (WH8103) (Cyanobacteria). J. Phycol. 43, 266–274.

Campestre, M.P., Bordenava, C.D., Origone, A.C., Menéndez, A.B., Ruiz, O.A., Rodríguez, A.A., Maiale, S.J., 2011. Polyamine catabolism is involved in response to salt stress in soybean hypocotyls. J. Plant Physiol. 168, 1234–1240.

Cohen, S.S., 1997. A Guide to the Polyamines. Oxford University Press, New York, USA.

Crosbie, N.D., Furnas, M.J., 2001. Abundance, distribution and flow-cytometric characterization of picophytoprokaryote populations in central (17°S) and southern (20 °S) shelf waters of the great barrier reef. J. Plankton Res. 23, 809–828.

Ducklow, H.W., Kirchman, D.L., Quinby, H.L., Carlson, C.A., Dam, H.G., 1993. Stocks and dynamics of bacterioplankton carbon during the spring bloom in the eastern North Atlantic Ocean. Deep-Sea Res. II 40, 245–263.

Gasol, J.M., Morán, X.A.G., 1999. Effects of filtration on bacterial activity and picoplankton community structure as assessed by flow cytometry. Aquat. Microb. Ecol. 16, 251–264.

Hamana, K., Matsuzaki, S., 1982. Widespread occurrence of norspermidine and norspermine in eukaryotic algae. J. Biochem. 91, 1321–1328.

Hamana, K., Matsuzaki, S., 1985. Further study on polyamines in primitive unicellular eukaryotic algae. J. Biochem. 97, 1311–1315.

Hamana, K., Niitsu, M., Hayashi, H., 2013. Occurrence of homospermidine and thermospermine as a cellular polyamine in unicellular chlorophyte and multicellular charophyte green algae. J. Gen. Appl. Microbiol. 59, 313–319.

Harrison, P.J., Zingone, A., Mickelson, M.J., Lehtinen, S., Ramaiah, N., Kraberg, A.C., Sun, J., McQuatters-Gollop, A., Jakobsen, H.H., 2015. Cell volumes of marine phytoplankton from globally distributed coastal data sets. Estuar. Coast. Shelf Sci. 162, 130–142.

Hosoya, R., Hamana, K., Isobe, M., Yokota, A., 2005. Polyamine distribution profiles within Cyanobacteria. Microbiol. Cult. Coll. 21, 3–8.

Hosoya, R., Yokoyama, Y., Hamana, K., Itoh, T., 2006. Polyamine analysis within the eubacterial thirteen phyla *Acidobacteria, Actinobacteria, Chlorobi, Chloroflexi, Chrysiogenetes, Deferribacteres, Fibrobacteres, Firmicutes, Fusobacteria, Gemmatimonadetes, Nitrospirae, Planctomycetes,* and *Verrucomicrobia*. Microbiol. Cult. Coll. 22, 21–33.

Incharoensakdi, A., Jantaro, S., Raksajit, W., Mäenpää, P., 2010. Polyamines in cyanobacteria: Biosynthesis, transport and abiotic stress response. In: Méndez-Vilas, A. (Ed.), Current Research, Technology and Education Topics in Applied Microbiology and Microbial Biotechnology. Formatex Research Center, Badajoz, pp. 23–32.

Keil, R.G., Mayer, L.M., Quay, P.D., Richey, J.E., Hedges, J.I., 1997. Loss of organic matter from riverine particles in deltas. Geochim. Cosmochim. Acta 61, 1507–1511.

Kirkham, A.R., Lepère, C., Jardillier, L.E., Not, F., Bouman, H., Mead, A., Scanlan, D.J., 2013. A global perspective on marine photosynthetic picoeukaryotes community structure. The ISME Journal 7, 922–936.

Knott, J.M., 2009. Biosynthesis of long-chain polyamines by crenarchaeal polyamine synthases from *Hyperthermus butylicus* and *Pyrobaculum aerophilum*. FEBS Lett. 583, 3519–3524.

Kotzabasis, K., 1994. Free, conjugated and bound polyamine during the cell cycling in synchronized cultures of *Scenedesmus obliquus*. Zeitschrift fur Naturforschung C 49, 181–185.

Kröger, N., Deutzmann, R., Bergsdorf, C., Sumper, M., 2000. Species-specific polyamines from diatoms control silica morphology. PNAS 97, 14133–14138.

Lee, C., Jørgensen, N.O.G., 1995. Seasonal cycling of putrescine and amino acids in relation to biological production in a stratified coastal salt pond. Biogeochemistry 29, 131–157.

Legendre, P., Legendre, L., 2012. Numerical ecology, , 3rd ednvol. 24. Elsevier, New York.

Lin, H.-Y., Lin, H.-J., 2019. Polyamines in microalgae: something borrowed, something new. Marine Drugs 17, 1.

Litchman, E., Klausmeier, C.A., Yoshiyama, K., 2009. Contrasting size evolution in marine and freshwater diatoms. PNAS 106, 2665–2670.

Liu, Q., Lu, X., Tolar, B.B., Mou, X., Hollibaugh, J.T., 2015. Concentrations, turnover rates and fluxes of polyamines in coastal waters of the South Atlantic bight. Biogeochemistry 123, 117–133.

Liu, Q., Nishibori, N., Imai, I., Hollibaugh, J.T., 2016. Response of polyamine pools in marine phytoplankton to nutrient limitation and variation in temperature and salinity. Mar. Ecol. Prog. Ser. 544, 93–105.

Liu, Q., Tolar, B.B., Ross, M.J., Cheek, J.B., Sweeney, C.M., Wallsgrove, N.J., Popp, B.N., Hollibaugh, J.T., 2018. Light and temperature control the seasonal distribution of thaumarchaeota in the South Atlantic bight. The ISME Journal 12, 1473–1485.

Lu, Y.H., Hwang, D.-F., 2002. Polyamine profile in the paralytic shellfish poison-producing alga *Alexandrium minutum*. J. Plankton Res. 24, 275–279.

Lu, X.X., Zou, L., Clevinger, C., Liu, Q., Hollibaugh, J.T., Mou, X.Z., 2014. Temporal dynamics and depth variations of dissolved free amino acids and polyamines in coastal seawater determined by high-performance liquid chromatography. Mar. Chem. 163, 36–44.

Makinen, C.P., Moisan, T.A.H., 2012. Phytoplankton assemblage patterns in the southern mid-Atlantic bight. Botanic Marina 55. https://doi.org/10.1515/bot-2012-0110.

Menden-Deuer, S., Lessard, E.J., 2000. Carbon to volume relationships for dinoflagellages, diatoms, and other protist plankton. Limnol. Oceanogr. 45 (3), 569–579.

Michael, A.J., 2016. Polyamine in eukaryotes, bacteria, and archaea. J. Biol. Chem. 291, 14896–14903.

Michael, A.J., 2018. Polyamine function in archaea and bacteria. J. Biol. Chem. 293 (48), 18693–18701.

Moisan, T.A., Blattner, K.L., Makinen, C.P., 2010. Influences of temperature and nutrients on Synechococcus abundance and biomass in the southern mid-Atlantic bight. Cont. Shelf Res. 30, 1275–1282.

Mou, X., Vila-Costa, M., Sun, S., Zhao, W., Sharma, S., Moran, M.A., 2011. Metatranscriptomic signature of exogenous polyamines utilization by coastal bacterioplankton. Environ. Microbiol. Rep. 3, 798–806.

Murrell, M.C., Hollibaugh, J.T., 2000. Distribution and composition of dissolved and particulate organic carbon in northern San Francisco Bay during low flow conditions. Estuar. Coast. Shelf Sci. 51, 75–90.

Nguyen, T.N.M., Berzano, M., Gualerzi, C.O., Spurio, R., 2011. Development of molecular tools for the detection of freshwater diatoms. J. Microbiol. Methods 84, 33–40.

Nishibori, N., Nishijima, T., 2004. Changes in polyamine levels during growth of a red-tide causing phytoplankton *Chattonella antiqua* (*Raphidophyceae*). Eur. J. Phycol. 39, 51–55.

Nishibori, N., Nishio, S., 1997. Occurrence of polyamines in the broom forming toxic dinoflagellate *Alexandrium tamarense*. Fish. Sci. 63, 319–320.

Nishibori, N., Yuasa, A., Sakai, M., Fujihara, S., Nishio, S., 2001. Free polyamine concentrations in coastal seawater during phytoplankton bloom. Fish. Sci. 67, 79–83.

Nishibori, N., Matuyama, Y., Uchida, T., Moriyama, T., Ogita, Y., Oda, M., Hirota, H., 2003. Spatial and temporal variations in free polyamine distributions in Uranouchi inlet. Japan. Mar Chem 82 (3), 307–314.

Nishibori, N., Fujihara, S., Nishijima, T., 2006. Changes in intracellular polyamine concentration during growth of *Heterosigma akashiwo* (*Raphidophyceae*). Fish. Sci. 72, 350–355.

Olson, R.J., Zettler, E.R., DuRand, M.D., 1993. Phytoplankton analysis using flow cytometry. In: Kemp, P.E., Sherr, B.F., Sherr, E.B., Cole, J.J. (Eds.), Handbook of

Methods in Aquatic Microbial Ecology. Lewis Publishers, Boca Raton, FL, pp. 175–186.
Partensky, F., Hess, W.R., Vaulot, D., 1999. Prochlorococcus, a marine photosynthetic prokaryote of global significance. Microbiology and Molecular Biology Review 63, 106–127.
Rocap, G., Larimer, F.W., Lamerdin, J., Malfatti, S., Chain, P., Ahlgren, N.A., Arellano, A., Coleman, M., Hauser, L., et al., 2003. Genome divergence in two Prochlorococcus ecotypes reflects oceanic niche differentiation. Nature 424, 1042–1047.
Sagor, G.H.M., Berberich, T., Takahashi, Y., Niitsu, M., Kusano, T., 2013. The polyamine spermine protects Arabidopsis from heat stress-induced damage by increasing expression of heat shock-related genes. Transgenic Res. 22, 595–605.
Saha, J., Brauer, E.K., Sengupta, A., Popescu, S.C., Gupta, K., Gupta, B., 2015. Polyamines as redox homeostasis regulators during salt stress in plants. Frontiers in Environmental Sciences 3, 21.
Schaefer, S.C., Alber, M., 2005. Trends in Agricultural Sources of Nitrogen in the Altamaha River Watershed. Georgia Institute of Technology.
Schweikert, K., Burritt, D.J., 2015. Polyamines in macroalgae: advances and future perspectives. J. Phycol. 51, 838–849.
Shah, P., Swiatlo, E., 2008. A multifaceted role for polyamines in bacterial pathogens. Mol. Microbiol. 68 (1), 4–16.
Shen, H.-J., Galston, A.W., 1985. Correlations between polyamine ratios and growth patterns in seedling roots. Plant Growth Regul. 3, 353–363.
Strathmann, R.R., 1967. Estimating the organic carbon content of phytoplankton from cell volume or plasma volume. Limnol. Oceanogr. 12, 411–418.
Sumper, M., Kröger, N., 2004. Silica formation in diatoms: the function of long-chain polyamines and silaffins. J. Mater. Chem. 14, 2059–2065.
Tabor, C.W., Tabor, H., 1985. Polyamines in microorganisms. Microbiol. Rev. 49, 81–99.
ter Braak, C.J.F., Smilauer, P., 2002. CANOCO Reference Manual and CanoDraw for Windows user's Guide: Software for Canonical Community Ordination (Version 4.5). Microcomputer Power, Ithaca.
Theiss, C., Bohley, P., Voigt, J., 2002. Regulation by polyamines of ornithine decarboxylase activity and cell division in the unicellular green alga *Chlamydomonas reinhardtii*. Plant Physiol. 128, 1470–1479.
Verity, P.G., Robertson, C.Y., Tronzo, C.R., Andrews, M.G., Nelson, J.R., Sieracki, M.E., 1992. Relationships between cell volume and the carbon and nitrogen content of marine photosynthetic nanoplankton. Limnol. Oceanogr. 37, 1434–1446.
Worden, A.Z., Not, F., 2008. Ecology and diversity of picoeukaryotes. In: Kirchman, D.L. (Ed.), Microbial Ecology of the Oceans, 2nd Edn. John Wiley & Sons, Hoboken, NJ, USA, pp. 159–205.
Worden, A.Z., Nolan, J.K., Palenik, B., 2004. Assessing the dynamics and ecology of marine picophytoplankton: the importance of the eukaryotic component. Limnol. Oceanogr. 49, 168–179.
Yamaguchi, K., Takahashi, Y., Berberich, T., Imai, A., Miyazaki, A., Takahashi, T., Michael, A., Kusano, T., 2006. The polyamine spermine protects against high salt stress in Arabidopsis thaliana. FEBS Lett. 580, 6783–6788.